Model
Error Resolution Document

Complete only applicable items.

QA: QA
Page 1 of 25

1. Document Number:	2. Revision/Addendum:	3. ERD:
ANL-EBS-MD-000033	06	03

4. Title:	5. No. of Pages Attached:
Engineered Barrier System: Physical and Chemical Environment	24

6. Description of and Justification for Change (Identify affected pages, applicable CRs and TBVs):

Justification for change:
This ERD was created to partially or totally resolve five Condition Reports, CR 13343, CR 13369, CR 13514, CR 13647, and CR 13655.

CR 13343 describes the use of incorrect fracture parameters in FEHM transport simulations used to calibrate the near field chemistry model. Simulations with the correct fracture parameters have been carried out using a different transport code, T2R3D, which more realistically models transport through the UZ. In this ERD, the calculations and results are documented, and an impact analysis comparing the new results and the original results is presented. The supporting calculations are included in a revision to an existing output DTN (DTN: SN0705PAEBSPCE.009) from the P&CE.

CR 13369 describes a minor error in Section 6.2.4.2, concerning a discussion of Table 6.6-1. The erroneous text is corrected in this ERD.

CR 13514 notes that Figure 6.6-8 of the P&CE is incomplete, and that the correct version is presented in the cited source DTN for the figure. The incorrect figure is replaced in this ERD.

CR 13647 describes three errors in the near field chemistry model description and pore water chemistry discussions in REV06 of the P&CE report, and in associated output DTNs, that are fixed here:

(1) On pages 6-186 and 6-187, in two locations, the text incorrectly cites a temperature of 96°C instead of 100°C. A calculation in one of the output DTNs from the P&CE makes the same error, and is also corrected.
(2) On page 6-87, the text refers to "...eight perched water samples..." The actual number of samples is nine.
(3) Lithologic unit assignments for perched water samples in output DTN SN0705PAEBSPCE.015 are corrected. This error does not affect text in the body of the P&CE report; the correction is only in the DTN.

CR 13655 notes that there is a repeated number in the axis numbering on Figures 7.1-6 and 7.1-7. The correct versions are presented in the cited source output DTN for the figures. The incorrect figures are replaced in this ERD.

Description of changes to Engineered Barrier System: Physical and Chemical Environment REV06, ERD03:
A detailed description of the changes is appended to this form.

	Printed Name	Signature	Date
7. Checker	Wendy Mitcheltree	Wendy Mitcheltree	9/24/09
8. QCS/QA Reviewer	Robert Spencer	Robert E Spencer	9/24/09
9. Originator	Charles R Bryan	Charles R Bryan	9/24/09
10. Responsible Manager	Palmer Vaughn	Palmer Vaughn	9/24/09

Detailed description of changes in response to CR 13343:

Section 3 (pages 3-1 to 3-3):

Replace this entire section with the following text. Note that this change is necessary both in response to CR 13343 and to correct the designation of Earthvision as qualified software instead of its current treatment as commercial off-the-shelf software.

3. USE OF SOFTWARE

The controlled software that was used to conduct the work described in this report is listed in Table 3.1-1 below. All qualified software discussed in this document was obtained from Software Configuration Management in accordance with IM-PRO-003, *Software Management*. All qualified software was used in the operating environments for which it was baselined. Qualified software was selected for use in this report because either it is the best available software for the modeling applications or is the only available software for the specific use. All qualified software selected is appropriate for the application and was only used within the range of validation in accordance with IM-PRO-003. Only standard functions were utilized, i.e., no macros or special software routines were developed for, or used by, the software selected. Note that GetEQData Version 1.0.1 is, itself, an Excel macro (see Table 3.1-1).

Commercial off-the-shelf software, including Microsoft Word, Microsoft Excel, Mathcad Versions 13 and 14, IGPET2006, Earthvision Version 5.1, JMP5.1, and Aq·QA Version 1.0, was employed to carry out this work (Table 3.1-2). This software is exempt from qualification per Section 2.0 of IM-PRO-003. The work was conducted using project standard desktop computers. Microsoft Word and Microsoft Excel are standard software applications used widely throughout the Yucca Mountain Project. They provide standard word processing and spreadsheet functions. There are no limitations on the use of the commercial off-the-shelf software used in this report related to their specified functions. No macros (other than GetEQData version 1.0.1 listed in Table 3.1-1) or special software routines were used by, or developed for, this software. Hand calculations or visual inspection of software outputs confirm that this software produces correct results. Note that, because the normative analysis performed by the IGPET2006 requires knowledge of petrology or mineralogy in order to follow the calculation, a hand calculation is included for reference as part of the documentation of the IGPET2006 data in Output DTN: SN0705PAEBSPCE.009. The use of each of these exempt software packages is documented in sufficient detail to allow a qualified person to reproduce and verify results. Earthvision 5.1 was used to extract average mineral abundances from the geologic framework model (DTN: MO0012MWDGFM02.002 [DIRS 153777]), as described in Section 4.1.5. The documentation of inputs and outputs related to the use of other exempt software is contained within the following DTNs: IGPET2006 as noted above; JMP5.1 and Aq. QA V.1.0 files are located in Output DTN: SN0705PAEBSPCE.015; Mathcad files are located in Output DTNs: SN0703PAEBSPCE.006 and SN0705PAEBSPCE.013; Excel files are located in all output and validation DTNs listed in Section 8.2.

Table 3.1-1. Qualified Software Used

Software	STN#	Platform/ OS	Limitations/Range of Use	Brief Description	Functions Utilized
EQ3/6 Version 8.0 [DIRS 162228]	10813-8.0-00	PC/ WIN2000	Temperature, pressure, and composition range determind by the input thermodynamic database	Thermodynamic speciation (EQ3NR) and solubility code, with reaction path capabilities (EQ6)	Standard functions
GetEQData Version 1.0.1 [DIRS 173680]	10809-1.0.1-00	PC/ WIN2000	Requires EQ3/6 V.8.0 or V.7.2b output files	Excel macro used to extract data from EQ3/6 V.8.0 output files	Data extraction
FEHM Version 2.24 [DIRS 178965]	10086-2.24-00	PC/ WIN2000	Used to perform one-dimensional, unsaturated zone flow and particle tracking transport calculations.	Finite element heat and mass transfer (FEHM) code for thermal-hydrologic calculations	Standard functions
ppptrk Version 1.0 [DIRS 165753]	11030-1.0-00	PC/ WIN2000	For use with particle tracking simulations only	Post-processor used to produce breakthrough curves from output files from FEHM particle tracking simulations	Data extraction and graphing
TOUGH2 Version 1.6 [DIRS 160242]	10007-1.6-00	Sun/OS 5.5.1	Used to perform one-dimensional, unsaturated zone flow calculations with AFM.	An integral finite difference numerical simulator for nonisothermal flows of multi-component, multiphase fluids in porous and fracture media	Standard functions
T2R3D Version 1.4 [DIRS 146654]	10006-1.4-00	Sun/OS 5.5.1	Used with TOUGH2 output files to perform one-dimensional, unsaturated zone transport calculations.	TOUGH2-based transport simulator for multicomponent, multiphase flows in porous and fracture media.	Standard functions.

Table 3.1-2. Exempt Software Used

Software	Platform/ OS	Limitations/Range of Use	Brief Description	Functions Utilized
Microsoft Word	PC/ WIN2000 or XP	No limitations; a common word processing program	Word processing	Standard functions
Microsoft Excel	PC/ WIN2000 or XP	No limitations; a common spreadsheet program	Spreadsheet software used to tabulate, calculate, analyze and visually display results	Standard functions
Mathcad version 13	PC/ WIN2000 or XP	No limitations; a common mathematics program	A standard engineering calculation software capable of advanced mathematics and graphing functions	Standard functions
Mathcad version 14	PC/ WIN2000 or XP	No limitations; a common mathematics program	A standard engineering calculation software capable of advanced mathematics and graphing functions	Standard functions
EARTHVISION 5.1	SGI/IRIX 6.2	Used for data extraction from the geologic framework model	A multiuse program for 3-D visualization of data and data extraction	Data extraction
IGPET2006	PC/ WIN2000 or XP	Used to compute normative analyses from bulk chemical data, requires oxide weight percent input	Applies the CIPW algorithm to whole rock analyses to compute a normative analysis	Algebraic functions standard to the program
JMP5.1	PC/ WIN2000 or XP	Used to conduct principal component analysis	A statistical analysis software package used to calculate PCA	Standard statistical functions
Aq·QA V.1.0	PC/ WIN2000 or XP	Used to compute and render Piper diagrams	Calculates chemical ratios and plots results on quaternary and ternary diagrams	Standard algebraic functions

Section 4.1:

The following direct inputs are added to Table 4.1-1, have modified Data/Parameter descriptions:

DTN or Document	Data/Parameter Description	Location in DTN or Report
LB990501233129.004 [DIRS 111475]	Geologic contacts used in FEHM and T2R3D simulations	File: *primary.mesh*, data corresponding to rock column "j34"
LB0205REVUZPRP.001 [DIRS 159525]	Fracture frequency (converted to fracture spacing, as 1/freq)	File: *FRACTURE_ PROPERTY.xls*
LB0207REVUZPRP.002 [DIRS 159672]	Matrix residual saturations	File: *Matrix_Props.xls*
SNL 2008 [DIRS 184748]	Distributions of effective permeability and fracture aperture used by the particle tracking model.	Table 6-8 (Group 3); Table 6-15 (Group 8)
	Fracture residual saturations	Section 6.5.6

Replace Section 4.1.11 with the following (note that this change is also associated with CR 14048, but only as an extent of condition for that CR which is not addressed directly in this ERD):

4.1.11 Stratigraphy and Hydrologic Properties Used in the FEHM and T2R3D Modeling

For the FEHM and T2R3D modeling, the geologic section at a specific location was used to model flow from the PTn/TSw boundary to the repository level, rather than the averaged values given in Table 4.1-7. Specific depths for stratigraphic contacts were taken from the model calibration grid for the three-dimensional (3-D) unsaturated zone (UZ) flow model, in project DTN: LB990501233129.004 [DIRS 111475] (file: *primary.mesh*, rock column "j34"; note that the repository is in the Tptpll unit at this location). This DTN was developed in an earlier version of *Development of Numerical Grids for Flow and Transport Modeling* (BSC 2004 [DIRS 169855]) and is unqualified. However, it is qualified for intended use in *Drift-Scale THC Seepage Model* (SNL 2007 [DIRS 177404], Appendix J). Because the same data (stratigraphic contacts and hydrostratigraphic unit thicknesses) are used in this report, the qualification in SNL 2007 ([DIRS 177404], Appendix J) is also applicable for this model report.

Relative permeability data (e.g., van Genuchten parameters) for the rock units intersected by the model were taken from qualified project DTN: LB0610UZDSCP30.001 ([DIRS 179180], File: *Calibrated Parameter_R113_30%.doc*); matrix and fracture porosities for the units are from the source given in Section 4.1.4.2 and presented in Table 4.1-6.

Additional parameters, used in the T2R3D model simulations, include matrix residual saturations, from qualified project DTN: LB0207REVUZPRP.002 ([DIRS 159672], File: *Matrix_Props.xls*); fracture residual saturations and distributions of effective permeability and fracture aperture, from Particle Tracking Model and Abstraction of Transport Processes (SNL 2008 [DIRS 184748], Section 6.5.6); and fracture spacing, from qualified project DTN: LB0205REVUZPRP.001 ([DIRS 159525], File: *FRACTURE_ PROPERTY.xls*). The actual parameter values are provided, and are discussed in detail, in Section 6.3.2.4.4.1.

Section 6.3.2.4.4 (page 6-45):

After the first paragraph of Section 6.3.2.4.4, (including Equations 6.3.17 and 6.3-18), insert the following text:

The plug-flow approximation is used to estimate the effective residence time of the *solute* in potential seepage water, rather than the water itself. The residence time for solvent water in the fractures is less than plug-flow estimates, and that for the rock matrix is greater. Plug flow approximates the effective residence time with respect to solute evolution in fracture water that can produce drift seepage. If inflowing fracture water at the top of the column were assigned the same composition as water in the matrix, then no compositional changes would occur in the column, and no breakthrough would be observed at the bottom. The breakthrough time thus expresses the average latency, or residence time, for any *difference* in composition of the inflowing water. The latency is caused by direct migration of solute into and out of the rock matrix, and the residence time approximates the time spent in the rock matrix. Conversely, it represents the time available for solutes that originate in the matrix to diffuse into the fractures, before breakthrough. In a slowly varying system that has achieved a dynamic steady state, the fracture and matrix water compositions are locally constant (but varying with depth); solute produced in the matrix (or net solute influx in the fractures) is transported to and from matrix and fractures by diffusion. The residence time at a particular location then corresponds to the average duration of transport from matrix and fractures (or vice versa) at the local, steady rate of production (or rate of net solute influx). The residence time for the stratigraphic column is obtained by integrating along the flow path. As discussed below, numerical simulations of tracer transport through the fractured host rock over a range of percolation fluxes were used for evaluating and calibrating the plug-flow approximation. Each simulation produces a breakthrough curve representing the change in concentration through time at the bottom of the rock column. Because fracture-matrix interaction is a spatially and temporally continuous process, the effect of matrix diffusion on the composition of seepage water is represented by a convolution of breakthrough times. The result is mixing of the effects from the upper and lower tails of the residence time distributions, in a manner that produces a net result that can be represented by the mean residence time.

Section 6.3.2.4.4 (page 6-46):

After the first paragraph below Table 6.3-1, insert the following text:

Application of numerical transport simulations for evaluating water-rock interaction and fracture-matrix interaction is consistent with studies in the technical literature, such as Johnson and DePaolo (1994 [DIRS 162560; 1996 [DIRS 162561]). The plug flow assumption used in the NFC model is similar to the porous medium approximation used by Johnson and DePaolo (1994 [DIRS 162560], p. 1580), which was used for evaluating transport through the unsaturated zone at Yucca Mountain.

Section 6.3.2.4.4 (pages 6-49 to 6-50):

The last three paragraphs in Section 6.3.2.4.4, starting with the paragraph with the bold-faced lead-in ***Evaluation of an Error in the FEHM Modeling Used to Calibrate the Percolation Flux Values****, will be replaced in total, with the following new subsection:*

6.3.2.4.4.1 Impact Evaluation for Errors in the Fracture Hydrologic Properties used in FEHM Transport Simulations

As described in Section 6.3.2.4.4, numerical simulations of tracer transport in the fractured host rock were used for calibrating the effective residence time approximation implemented in the NFC model. This approximation represents residence time of the solute in potential seepage water, rather than the water itself. Plug-flow is an aggregation of fast and slow pathways that implies physical and chemical equilibrium between the pathways. For the NFC model, "plug-flow" is implemented by choosing a percolation flux that produces the effective residence time calculated from numerical transport simulations. The residence time for solvent water in the fractures is less than the effective residence time for solute, and the residence time for solvent water in the rock matrix is greater than the effective residence time for solute. The breakthrough time thus expresses the average latency that occurs for any difference in composition of the inflowing water. The transport simulations described in Section 6.3.2.4.4 were performed using FEHM V2.24 (STN: 10086-2.24-00, [DIRS 178965]) in a manner similar to 1-D validation cases used in support of the abstraction of UZ transport for TSPA (SNL 2008 [DIRS 177396], Figures 7-2 through 7-7).

However, some fracture hydrologic parameters (the fracture spacing and permeability) used in the TSPA baseline FEHM simulations in Section 6.3.2.4.4 are incorrect; also, the active fracture model (AFM) implemented in other Yucca Mountain Project UZ transport models as not implemented. This section presents simulations carried out with T2R3D V1.4 (STN: 10006-1.4-00, [DIRS 146654]) that correct these errors. The T2R3D code was selected for these analyses because it implements a more comprehensive version of AFM than does FEHM; it incorporates the AFM in both flow and transport using full numerical implementation of the differential equations for flow and transport, while FEHM only implements AFM for transport calculations. These simulations therefore address both the errors in the fracture hydrologic parameters in the original FEHM calculations, and the effect of not considering AFM.

To evaluate the effects of these errors on the potential seepage water compositions predicted by the near field chemistry model, transport simulations were performed with T2R3D using corrected fracture hydrologic parameters. Then, the predicted mean breakthrough times were used to recalibrate the plug flow transport times used in the near field chemistry model calculations for the TSPA. A new WRIP map was generated, and water chemistries calculated using the new WRIP map are compared to those calculated using the TSPA WRIP map.

T2R3D Simulations of Transport Times Through the TSw using AFM

Calculation of the effective residence time, or "plug-flow transport time," and the associated velocity is described earlier in Section 6.3.2.4.4 of this model report. The key transport and hydrologic parameters of these simulations are shown in Tables 6.3-4a and 6.3-4b. The T2R3D simulations used the same transport and hydrologic properties as the FEHM simulations, including the same geologic column and unit thicknesses (Section 4.1.11), relative permeability data (e.g., van Genuchten parameters) for units intersected by the model (Section 4.1.11), matrix and fracture porosities (Section 4.1.4.1).

Table 6.3-4a. Transport Parameters for FEHM and T2R3D Simulations used with the NFC Model

Hydrologic Unit	Unit Bottom Elevation (m)	Unit Top Elevation (m)	Unit Thickness (m)	Fracture Spacing (m)	Active Fracture γ[1]
tsw31	1,279.7	1,294.1	14.4	0.46	0.4[2]
tsw32	1,249.3	1,279.7	30.4	0.89	0.4
tsw33	1,169.2	1,249.3	80.1	1.23	0.4
tsw34	1,132.0	1,169.2	37.2	0.23	0.4
tsw35	1,030.6	1,132.0	101.4	0.32	0.4

SOURCES: DTN: LB990501233129.004 [DIRS 111475], File: *primary.mesh*, rock column "j34" — geologic column:
DTN: LB0205REVUZPRP.001 [DIRS 159525] File: *FRACTURE_ PROPERTY.xls*— fracture spacing (1/freq.).

NOTES: 1. Sensitivity analyses varied the AFM γ parameter between values of zero (all fractures accessible), 0.4, and 0.8.
2. The value of γ = 0.4 for the tsw31 unit is used in this response for consistency with the original FEHM simulations described in Section 6.3.2.4.4. A value of γ = 0.088 is used for corresponding simulations with the UZ flow model (SNL 2007 [DIRS 184614], Table B-2).

Table 6.3-4b. Hydrologic Properties for All FEHM and T2R3D Simulations Presented

Hydrologic Unit	Fracture Porosity	Fracture Permeability (m^2)	α_F (m^{-1})	vG n_F	Fracture Residual Saturation	Matrix Porosity	Matrix Permeability (m^2)	α_M (m^{-1})	vG n_M	Matrix Residual Saturation
tsw31	0.0050	8.1×10^{-13}	0.204	2.7248	0.01	0.043	3.21×10^{-17}	0.284	1.272[1]	0.21
tsw32	0.0083	7.1×10^{-13}	0.554	2.7248	0.01	0.146	3.01×10^{-16}	0.156	1.408	0.07
tsw33	0.0058	7.8×10^{-13}	15.5	2.7248	0.01	0.136	1.86×10^{-17}	0.064	1.395	0.12
tsw34	0.0085	3.3×10^{-13}	3.10	2.7248	0.01	0.090	3.16×10^{-18}	0.0168	1.464	0.19
tsw35	0.0096	9.1×10^{-13}	5.64	2.7248	0.01	0.115	1.11×10^{-17}	0.0331	1.276	0.12

SOURCES: DTN: LB0610UZDSCP30.001 [DIRS 179180], File: *Calibrated Parameter_R113_30%.doc* — matrix/fracture permeabilities and van Genuchten parameters
DTN: LB0208UZDSCPMI.002 [DIRS 161243] File: *drift-scale calibrated properties for mean infiltration2.xls* — matrix and fracture porosities.
DTN: LB0207REVUZPRP.002 [DIRS 159672] File: *Matrix_Props.xls* — matrix residual saturations
SNL (2008 [DIRS 184748], Section 6.5.6) — fracture residual saturations

NOTES: Parameters for the van Genuchten (1980) equation for capillary pressure in the matrix (α_M and n_M) and fractures (α_F and n_F) are derived from those in the source DTN (m and $\alpha(Pa^{-1})$) by simple mathematical transforms: n = 1/(1-m) and $\alpha(m^{-1})$ = 1000 (kg m^3) * 9.81 (m s^{-2}) * $\alpha(Pa^{-1})$
1. A value of 1.279 is used in the UZ flow model and for the T2R3D simulations presented in this response.

As with the FEHM simulations, the active fracture γ was assumed to be 0.4 for all units. A matrix diffusion coefficient of 3.47×10^{-11} m^2/s was used for all units, in both the original FEHM simulations and the new T2R3D simulations. Fracture residual saturations were taken to be 0.01 to be consistent with *Particle Tracking Model and Abstraction of Transport Processes* (SNL 2008 [DIRS 184748], Section 6.5.6). Matrix residual saturations are from DTN: LB0207REVUZPRP.002 ([DIRS 159672], File: *Matrix_Props.xls*).

The error in the original FEHM simulations was in the fracture permeabilities that were used. The fracture permeabilities were those listed in Table 6.3-4b, which are from the UZ calibrated properties set. In the UZ calibrated properties set, "fracture permeability" is the bulk permeability of the fracture continuum. However, in FEHM, "fracture permeability" is the permeability of an individual fracture; it must be multiplied by the fracture volume fraction to represent the bulk permeability of the fracture continuum. The value that should have been used in the original FEHM simulations was the permeability value from the UZ calibrated properties set *divided by the fracture volume fraction*. Hence, the fracture permeabilities used in the FEHM simulations were about two orders of magnitude too low, resulting in higher fracture saturations and somewhat longer transport times. The new T2R3D simulations discussed here use the appropriate fracture permeability values for each of the rock units in the hydrostratigraphic section.

As with the original FEHM simulations, the T2R3D simulations were carried out at percolation fluxes 1, 3, 10, 30, and 100 mm/yr, thereby addressing the impact of variable flow rates. Trend extrapolation is used in the NFC model for limited application to percolation flux values greater than 100 mm/yr (Section 6.3.2.4.4). At higher percolation fluxes, extrapolation results in larger relative uncertainty in transport times; however, the degree of water-rock interaction is so low at fluxes greater than 100 mm/yr that the effect of the extra uncertainty on predicted water composition is negligible. All of the simulations were performed with zero longitudinal and transverse dispersivities, which is appropriate given that matrix diffusion has a much greater effect on tracer transport than does dispersion (Zhou et al. 2003 [DIRS 162133], p. 25).

For these new simulations, the flow calculations were performed using TOUGH2 v1.6 (STN: 10007-1.6-00, [DIRS 160242]) with the eos9 module for single-phase, unsaturated, isothermal flow. Steady-state flow fields were computed by carrying out a transient flow simulation to 10 million years from a set of assumed initial conditions with steady-flow boundary conditions. The steady flow fields were confirmed by a constant total flux throughout the column. The transport calculations were carried out using the TOUGH2-compatible transport simulator, T2R3D. Transport calculations were conducted using steady-state flow fields computed from TOUGH2 and specifying an initial tracer mass in the top fracture cell. The TOUGH2 and T2R3D input and output files are archived in Output DTN: SN0705PAEBSPCE.009, folder *T2R3D sensitivity analysis\T2R3D simulations*; see the DTN readme file for an explanation of the file structure and a description of the file naming conventions.

Breakthrough curves predicted with T2R3D are compared with the original FEHM breakthrough curves in Figure 6.3-7a and in Table 6.3-4c. Calculated plug flow transport times are also shown. Remember, however, that within the near field chemistry model, percolation fluxes are adjusted until the calculated plug flow transport times are equal to the log-normal mean values from the FEHM breakthrough curves; because the FEHM breakthrough curves are symmetrical in log space, this is essentially equivalent to the median value (Figure 6.3-7). As shown in Figure 6.3-7a and Table 6.3-4c, breakthrough times for the T2R3D simulations are similar to the FEHM results up to a percolation flux of approximately 10 mm/yr, and then decrease relative to the FEHM results for flux greater than 10 mm/yr. The breakthrough curves in Figure 6.3-7a are distributions of tracer residence time for the boundary condition of instantaneous fracture release—a pulse into the fracture continuum at the top of the column. "Tailing" of the breakthrough curves increases for simulations at higher flux values. This dispersive "tailing" is caused mostly by the retarding effect of matrix diffusion, although T2R3D contributes a small amount of numerical dispersion that is not evident in the FEHM particle tracking results. Residence time dispersion is not significant to the use of calculated mean residence times from these curves, because fracture-matrix interaction is a spatially and temporally continuous process as discussed previously.

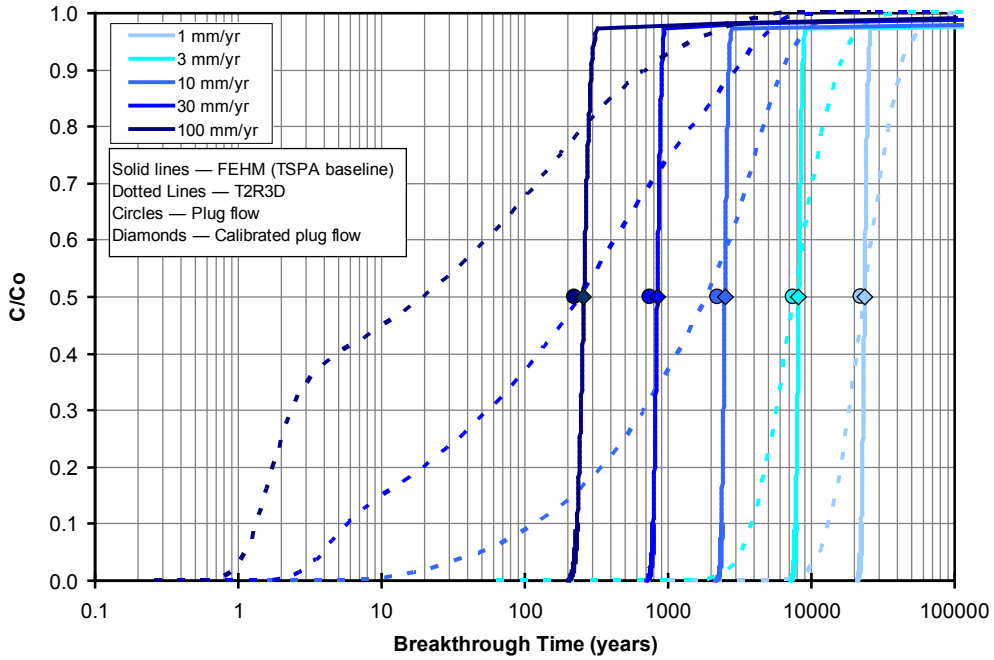

Source: Output DTN: SN0705PAEBSPCE.009, File: T2R3D impact analysis\T2R3D runs*T2-FEHM pulse release comparison.xls*.

Figure 6.3-7a. Original FEHM Breakthrough Simulations and Recalculated T2R3D Simulations (γ = 0.4) with Instantaneous Pulse Release in Fractures at the Top of the Column, and Fluxes of 1, 3, 10, 30, and 100 mm/yr, Plotted with Calibrated and Uncalibrated Plug-Flow Points from NFC Model.

Table 6.3-4c. Effective Residence Time Calibration with FEHM and T2R3D Transport Simulations

Percolation Flux (mm/yr)	Plug-Flow Residence Time Based on Percolation Flux (yr)	Calibrated Using Original FEHM Runs (TSPA-LA) (yr)	T2R3D Recalculated Median Residence Time (yr)	Difference of Recalculated vs. Original Calibrated Results (%)
1	22,224	23,484	23,578	0.4
3	7,408	8,170	7,626	−6.7
10	2,222	2,494	1,871	−25.0
30	741	840	241	−71.3
100	222	258	19	−92.6

Sources: FEHM and plug flow results: Output DTN: SN0703PAEBSPCE.007, File: *Transport time uncertainty.xls*.

T2R3D results: Output DTN: SN0705PAEBSPCE.009, File: T2R3D impact analysis\Seepage water chemistry\ *Median_BT_Times.xmcd*.

Impact Evaluation for Recalculated Residence Times

The impact of adjusting the effective residence times in the NFC model using the T2R3D simulations is limited because the greatest relative difference (percent change in Table 3) is associated with higher flux conditions for which water-rock interaction is small relative to lower percolation flux conditions. To evaluate the impact on in-drift chemistry, median values for the T2R3D breakthrough curves were used to recalibrate the effective residence times in the NFC model (i.e., the percolation flux values used in a "plug-flow" calculation), and the NFC model was rerun using the new percolation flux values to generate a new response surface for the water–rock interaction parameter (the WRIP "map"). The calculation of the amount of feldspar dissolved and the generation of the WRIP map is discussed in Section 6.3.2.4.5. That procedure was modified for this impact analysis, as discussed in detail below (unless otherwise specified, these calculations are captured in Output DTN: SN0705PAEBSPCE.009, Folder: T2R3D impact analysis\Seepage water chemistry):

- The median breakthrough times were calculated by fitting the measured data with a cubic spline function and interpolating to determine the time corresponding to a breakthrough concentration of 0.5 (*Mean_BT_Times.xmcd)*. Median breakthrough times were used instead of mean breakthrough times as was done originally for the NFC model because the means for the T2R3D breakthrough curves at higher flux values are skewed to larger values by "tailing" behavior. The choice of median values is more consistent with the dynamic-steady state assumption inherent to the effective residence time approximation.

- The percolation fluxes used in the plug flow model were calibrated such that the predicted residence times matched the median breakthrough times in the T2R3D simulations. (*Transport time uncertainty, T2R3D simulations.xls*). This was done in a similar manner to that described in Section 6.3.2.4.4, by modifying the spreadsheet used to calibrate to the original FEHM breakthrough curves.

- The three original near field chemistry model Mathcad files for evaluating water-rock interactions (Output DTN: SN0703PAEBSPCE.006, Folder: WRIP calculations\ Mathcad calculations of WRIP values) were modified to include the new percolation fluxes and rerun, using the original data for the thermal field, as that part of the model did not change. Then, a revised WRIP map was assembled from the outputs of these three simulations (*WRIP lookup table T2R3D.xls*).

- Using GetEQData V. 1.0.1, seepage composition as a function of WRIP value and drift wall temperature were extracted from the Group 3 EQ3/6 seepage simulations used to generate the pickup files for the seepage evaporation abstraction (Output DTN: SN0701PAEBSPCE.002, Folder: PCE-DTN-2\EQ3_6 seepage\Gp3). The extracted data are compiled in Output DTN: SN0705PAEBSPCE.009 File: T2R3D impact analysis\Seepage water chemistry\Mathcad calcs, chemistry*GP-3 seepage lookup tables.xls*.

- The predicted drift wall temperature history for the highest thermal measure in the WRIP map was identified. This corresponds to Drift 7, Position 11, for the 10th percentile thermal conductivity simulations (Output DTN: SN0703PAEBSPCE.006, file: WRIP calculations\Mathcad calculations of WRIP values\thermal-K, 10th percentile*Drift 7.xls*, tab "Results", line 164). Using the thermal history corresponding to the highest thermal measure results to the largest amount of water-rock interaction, and also in the greatest difference in chemistries predicted using the baseline simulations and the new results calculated using the T2R3D breakthrough times. Differences will be less at any lower thermal measure.

- Utilizing Mathcad, the drift wall temperature history for the highest thermal measure and the WRIP values for that thermal measure (a matrix consisting of 102 rows representing time steps by 20 columns representing sets of percolation flux histories), were then used to sample seepage compositions from the extracted Group 3 seepage chemistry data. The same procedure was followed for both the original WRIP map used in the TSPA-LA, and the new map generated with T2R3D results. These Mathcad calculations are in file *NFC Chemistry, Gp3, high.xmcd*; the results were copied to *GP-3_Chemistry-Compare.xls* for plotting (Output DTN: SN0705PAEBSPCE.009, Folder: T2R3D impact analysis\ Seepage water chemistry\Mathcad calcs, chemistry).

The results are shown in Figure 6.3-7b, which compares the compositions of seepage water through time, for selected percolation flux histories in the WRIP map, for the hottest waste package location in the repository as represented for the NFC model. Potassium and calcium concentrations and pH are shown, because potassium and calcium concentrations show greater relative change compared to other aqueous components, and because pH is an important parameter with respect to TSPA. Moreover, these are species that are affected by water-rock interaction, whereas conservative species such as chloride are not affected. The percolation flux histories plotted in Figure 6.3-7b correspond to those in Table 6.3-1.

Examination of Figure 6.3-7b indicates that, at low percolation flux values, for which breakthrough times are similar to values used for the TSPA-LA, there is little difference in predicted water chemistry between the original FEHM results (dotted lines) and the T2R3D results (solid lines). For percolation flux histories 1 and 2, the dotted and solid lines are superposed. Differences in key chemical species increase at higher flux values (above 10 mm/yr) during the thermal pulse, but are limited to a few parts per million in concentration (or a small fraction of a pH unit). At a later time during repository cooling, the differences decrease significantly. At the highest percolation flux values (30 mm/yr and higher), there is relatively little reaction between the rock and the downward moving water, although the effects of heating (e.g., calcite precipitation) are still observed.

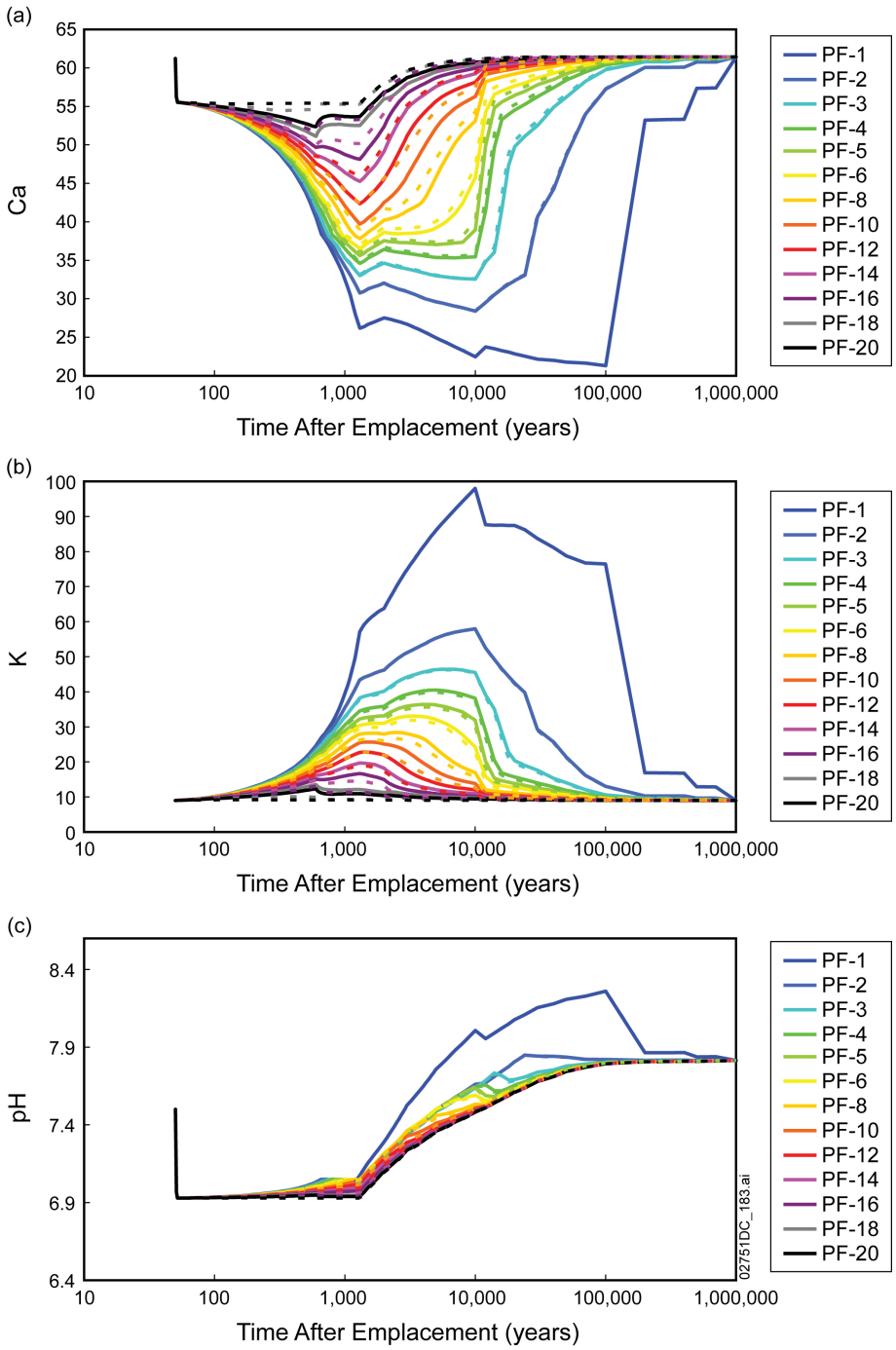

Source: Output DTN: SN0705PAEBSPCE.009, File: T2R3D impact analysis\Seepage water chemistry\Mathcad calcs, chemistry*GP-3_Chemistry-Compare.xls*.

NOTE: Solid lines represent the original results used in the TSPA-LA, and dotted lines are results using T2R3D. "PF" refers to percolation flux histories 1 through 20, used in the NFC model. Percolation flux histories are given in Table 6.3-1. Units for chemical species K and Ca are mg/L.

Figure 6.3-7b. Comparison of Seepage Water Compositions using the NFC Model with Adjusted Residence Time Based on Recalculated T2R3D Simulations for: (a) Calcium, (b) Potassium, and (c) pH

This comparison shows that the incorrect specifications for the fracture parameters in the FEHM simulations described in Section 6.3.2.4.4, and the use of non-AFM flow and transport simulations in the TSPA baseline near field chemistry model, have little effect on the composition of potential seepage water. Concentrations of chemical constituents changed by a few mg/L, and the impact is limited to the duration of the thermal pulse. These results show that the plug-flow feature of the NFC model, when calibrated to numerical results that include rapid breakthrough behavior at higher percolation flux values, is a reasonable approximation for the effective residence time or transport velocity of solute in waters percolating through the host rock.

Sensitivity Analyses for Transport Parameters

Additional sensitivity analyses were carried out to evaluate sensitivity to important parameters and modeling choices in the flow and transport modeling for the near field chemistry model. Specifically, three sensitivity analyses were carried out:

- T2R3D simulations in which the initial tracer mass was distributed uniformly throughout all matrix cells. These are termed "global matrix release" in the following discussion, and offer insights into the rate of diffusive equilibration of matrix and fracture waters relative to downward transport.

- Simulations in which the sensitivity to the AFM gamma (γ) value is evaluated. This parameter accounts for flow focusing in the UZ by limiting the wetted fracture area to a fraction of the total matrix-fracture contact area. In the TOUGH2/T2R3D simulations discussed here, this parameter affects both the flow field and the transport calculations.

- Simulations in which the sensitivity to the effective matrix diffusion coefficient is evaluated.

The TOUGH2 and T2R3D input and output files for these simulations are archived in Output DTN: SN0705PAEBSPCE.009, folder: T2R3D sensitivity analysis\T2R3D simulations. See the DTN readme file for an explanation of the file structure and a description of the file naming conventions.

Global matrix release—Results for instantaneous, global release of tracer throughout the matrix (instead of in the fractures at the top of the column) are shown in Figure 6.3-7c, with the baseline FEHM and TOUGH2 – T2R3D cases already discussed. The global matrix release cases represent behavior of solutes that include sodium and potassium ions that originate predominantly in the matrix and diffuse into fracture waters. Breakthrough for the matrix release simulations should be similar to the fracture release (top of column) cases because of reciprocity in solute diffusion behavior. Global release to matrix results in all tracer being delayed in the rock matrix but also initiates tracer release throughout the column. Thus, the tracer released globally throughout the matrix is closer to the bottom of the column, on average. These opposing effects can be seen in Figure 6.3-7c.

The diffusive transport time scale is proportional to $d_{fm}/D_m A_{fmv}$, where D_m is the matrix diffusion coefficient, d_{fm} is the fracture-matrix interface length scale, and A_{fmv} is the fracture-matrix interface area per unit volume. A Peclet number (P) for the process is defined by $P = q_f/(\phi_m S_m D_m A_{fmv})$, where q_f is the fracture flux, and ϕ_m is the matrix porosity. The average Peclet numbers for the 1, 10, and 100 mm/yr cases are about 1.09, 24.9, and 294, respectively (DTN: SN0705PAEBSPCE.009, File: T2R3D impact analysis\T2R3D runs\Sensitivity

analyses*Peclet.xls*). These show that as percolation flux increases, transport is more and more dominated by advective processes. At 1 mm/yr the diffusive time scale is short relative to the advective time scale, therefore, tracer released at the same elevation in fracture or matrix will tend to produce similar breakthrough times. However, for global matrix release, tracer is released closer to the end of the column on average, so this case shows earlier breakthrough than the fracture release case (Figure 6.3-7c). At 100 mm/yr, the diffusion time scale is long relative to the advection time scale, leading to longer breakthrough times for the global matrix release case compared with the fracture release case (Figure 6.3-7c). At 10 mm/yr, the effects of release location and relative transport rates balance such that the breakthrough curves for fracture release and global matrix release are similar (Figure 6.3-7c).

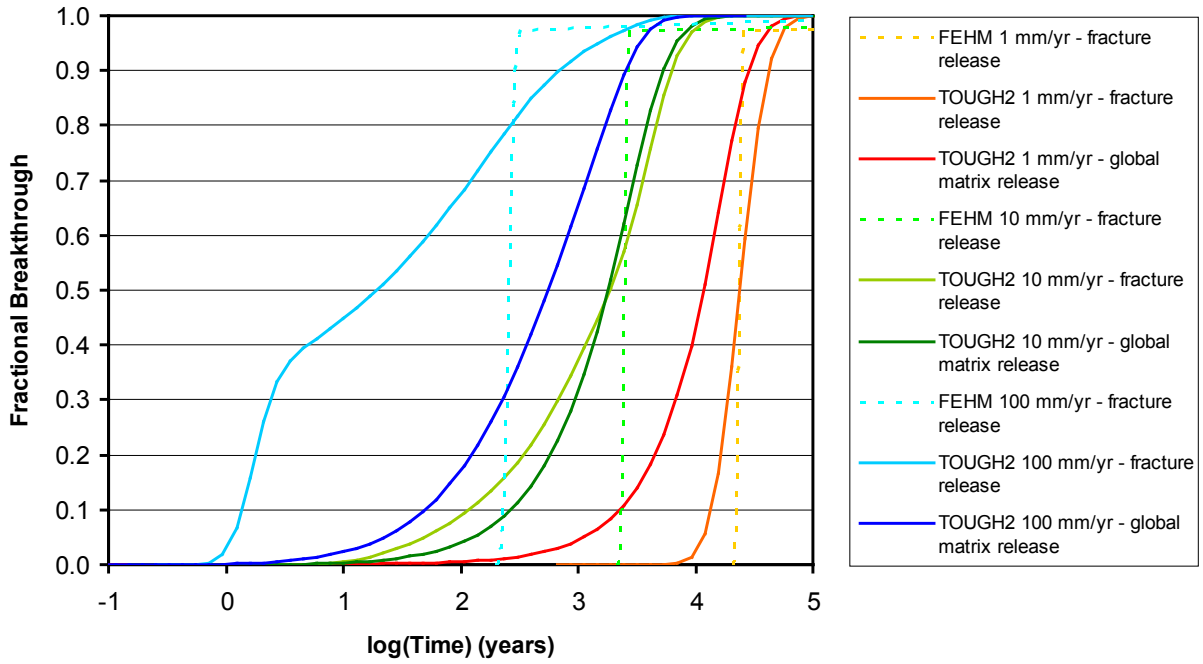

Source: Output DTN: SN0705PAEBSPCE.009, File: T2R3D impact analysis\T2R3D runs\Sensitivity analyses*Fracture vs global matrix release.xls*.

Figure 6.3-7c. T2R3D breakthrough curves for fracture and "global" matrix pulse releases, for flux values of 1, 10, and 100 mm/yr, with $\gamma = 0.4$.

Sensitivity to Gamma—Sensitivity calculations were performed as one-off cases from the baseline described in Section 6.3.2.4.4 at 10 and 100 mm/yr, as shown in Figure 6.3-14d. Two bounding fracture-matrix exchange conditions were investigated; the full interface case and a high active fracture parameter ($\gamma = 0.8$) case. The full interface sensitivity does not implement the AFM in any way. In this case, for both flow and transport, fracture flow is assumed to occur throughout the entire population of connected fractures and completely wets the fracture-matrix interface area. Therefore, the wetted interface area and distance from the matrix to the fracture-matrix interface remain constant, as established by the geometric fracture-matrix interface properties, for all fracture flow conditions. This case is representative of the maximum fracture-matrix interaction that could be expected. The $\gamma = 0.8$ case represents a high degree of flow focusing in the subset of connected fractures that participate in flow and transport processes. A value of $\gamma = 0.8$ is substantially higher than the range implemented in TSPA, ($\gamma = 0.2$ to 0.6) and is used here as a bounding case for limited fracture-matrix interaction. The baseline cases with

$\gamma = 0.4$ are also presented in Figure 6.3-7d, and are more representative. The results shown in Figure 6.3-7d indicate that the range in fracture-matrix interface conditions can result in initial breakthrough that ranges by more than two orders of magnitude, but has less effect on the trailing portion of the breakthrough curve.

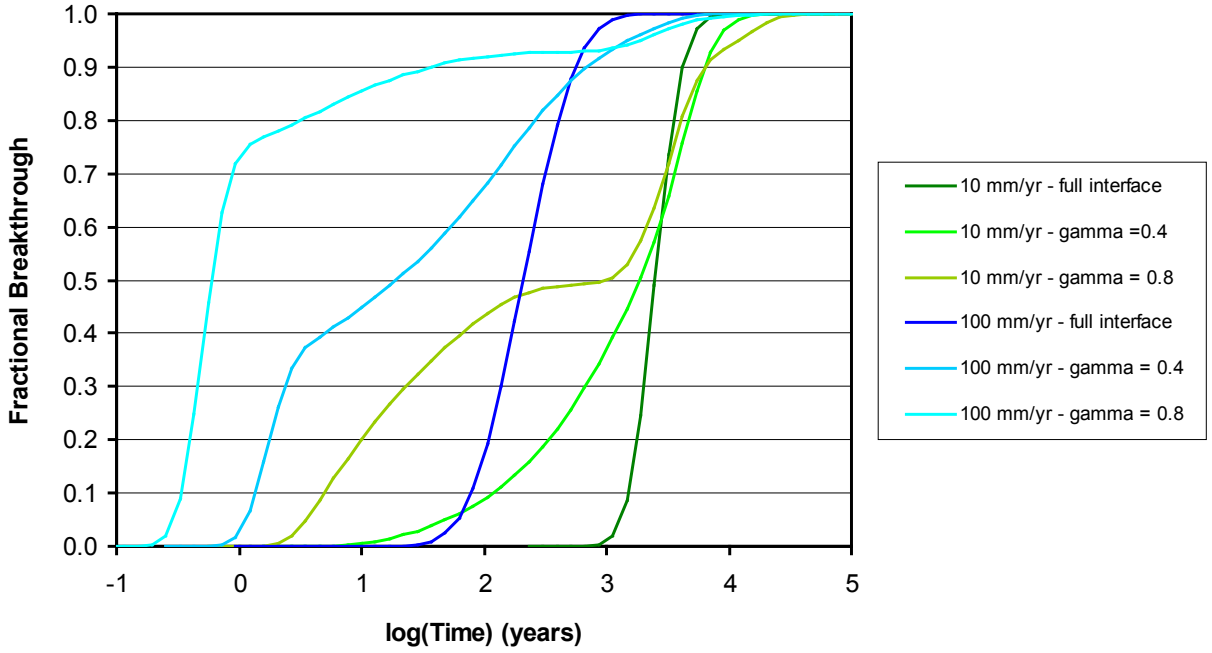

Source: Output DTN: SN0705PAEBSPCE.009, File: T2R3D impact analysis\T2R3D runs\Sensitivity analyses*Sensitivity to active fracture model gamma.xls*.

Figure 6.3-7d. T2R3D simulations (pulse fracture release) showing influence of the AFM γ parameter, with full interface and $\gamma = 0.4$, and 0.8, at percolation fluxes of 10 and 100 mm/yr.

Sensitivity to matrix diffusion coefficient—Two key uncertain parameters of matrix diffusion in the UZ transport model, besides the AFM gamma parameter, are the effective matrix diffusion coefficient (D_m) and fracture aperture ($2b$). Uncertainties for these and other parameters of the UZ transport model have been analyzed in detail (SNL 2008 [DIRS 184748], Section 6.5). A larger value for the effective matrix diffusion coefficient enhances fracture-matrix interaction, whereas a smaller value of fracture aperture enhances fracture-matrix interaction by increasing the effect of matrix diffusion on the rate of change of fracture water composition (Sudicky and Frind 1982 [DIRS 105043], Equation 1). The parameter analyses for UZ transport are used here to represent the effect of parameter uncertainty on the matrix diffusion results.

Assuming that the welded host-rock units above the repository (hydrostratigraphic units tsw31, tsw32, and tsw33) have similar properties to the units hosting most of the repository (tsw34 and tsw35), parameter uncertainties were evaluated for host-rock groups (SNL 2008 [DIRS 184748], Table 6-8, Group 3; also Table 6-15, Group 8). Using the tabulated data for group properties, discrete distributions for D_m and $2b$ were developed from the parametric distributions for substituent parameters. The 10^{th} and 90^{th} percentile values for these distributions vary within a factor of approximately two from the mean values. The parameters vary independently as sampled for TSPA, so a factor of two was selected for evaluating parameter uncertainty in breakthrough behavior. A set of breakthrough curves was calculated for a range of percolation flux (Figure 6.3-7e), indicating the extent of parameter uncertainty on fracture-matrix interaction.

The comparison with fracture-only transport shows that at 100 mm/yr, a significant front develops associated with fracture-only transport that is stronger at lower rates of matrix diffusion. The corresponding front at 10 mm/yr is practically undetectable (in terms of median transport times) over the same range of uncertainty in the matrix diffusion coefficient.

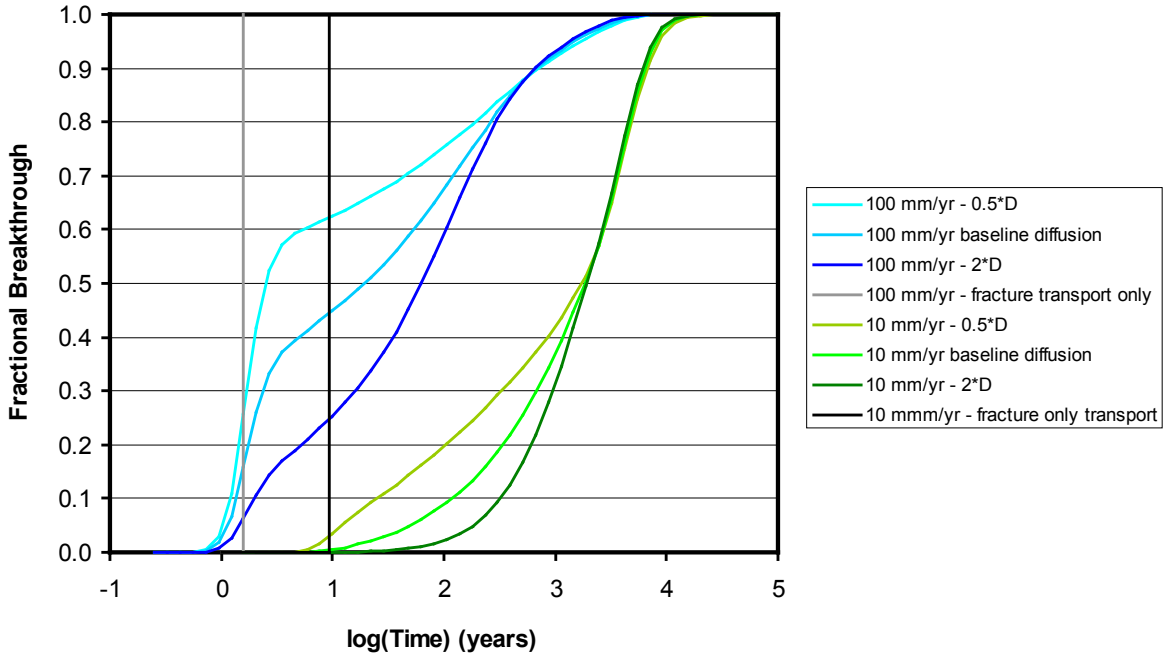

Source: Output DTN: SN0705PAEBSPCE.009, File: T2R3D impact analysis\T2R3D runs\Sensitivity analyses*Sensitivity to effective matrix diffusion coefficient.xls*.

Figure 6.3-7e. T2R3D breakthrough curves for fracture pulse releases, for a range of values for the matrix diffusion coefficient (Dm), for flux values of 10 and 100 mm/yr, and γ = 0.4.

Summary

The effect of fast fracture-flow pathways on fracture-matrix interaction is represented using the AFM. Calculated tracer breakthrough time is equivalent to an effective residence time for fracture-matrix interaction. The extent of water–rock interaction is represented in the near field chemistry model using an effective residence time approximation, calibrated to numerical simulations of tracer breakthrough. This approach is based on a dynamic-steady state assumption, and is an appropriate simplification that has been used previously in the technical literature. In this sensitivity analysis, breakthrough curves were calculated using the T2R3D code to correct errors in the specification of fracture parameters in the original FEHM simulations (Section 6.3.2.4.4) and to use the AFM in both flow and transport calculations. These breakthrough curves were then used to recalibrate effective residence time in the NFC model. An evaluation of the impact on the predicted chemistry of seepage waters from using the recalculated curves shows that use of the original FEHM breakthrough times results in overprediction of the degree of water-rock interaction. However, use of the corrected T2R3D breakthrough times results in concentration changes of only a few mg/L, and the impact is limited to higher percolation fluxes and to the duration to the thermal pulse. These changes are not significant relative to the overall range of waters predicted by the near field chemistry model.

Additional sensitivity analyses varying the AFM gamma parameter, the effective diffusion coefficient, and the mode of release, confirm that the plug-flow feature of the NFC model, when

calibrated to numerical results that include rapid breakthrough behavior at higher percolation flux values, is a reasonable approximation for the effective residence time or transport velocity of solute in waters percolating through the host rock.

Detailed description of changes in response to CR 13369:

Section 6.2.4.2 (page 6-17):

Replace:

Table 6.6-1 shows the composition of analyzed minor and trace elements in the pore waters extracted from cores collected in the TSw. As can be seen from Table 6.6-1, Pb and Hg concentrations and more than one-third of the arsenic concentrations are below the detection limits or not reported.

With:

Table 6.6-1 lists DTN sources for compositional data for pore waters extracted from cores collected in the TSw. Although minor and trace element components of the waters were not always measured, survey of the data in these DTNs shows that, when measured, Pb and Hg concentrations and more than one-third of the arsenic concentrations were below the detection limits of the method used (see, for example, data in DTN: GS020408312272.003).

Detailed description of changes in response to CR 13514:

Section 6.6.3, Figure 6.6-8 (page 6-97):

Replace the existing Figure 6.6-8, including notes and caption, with:

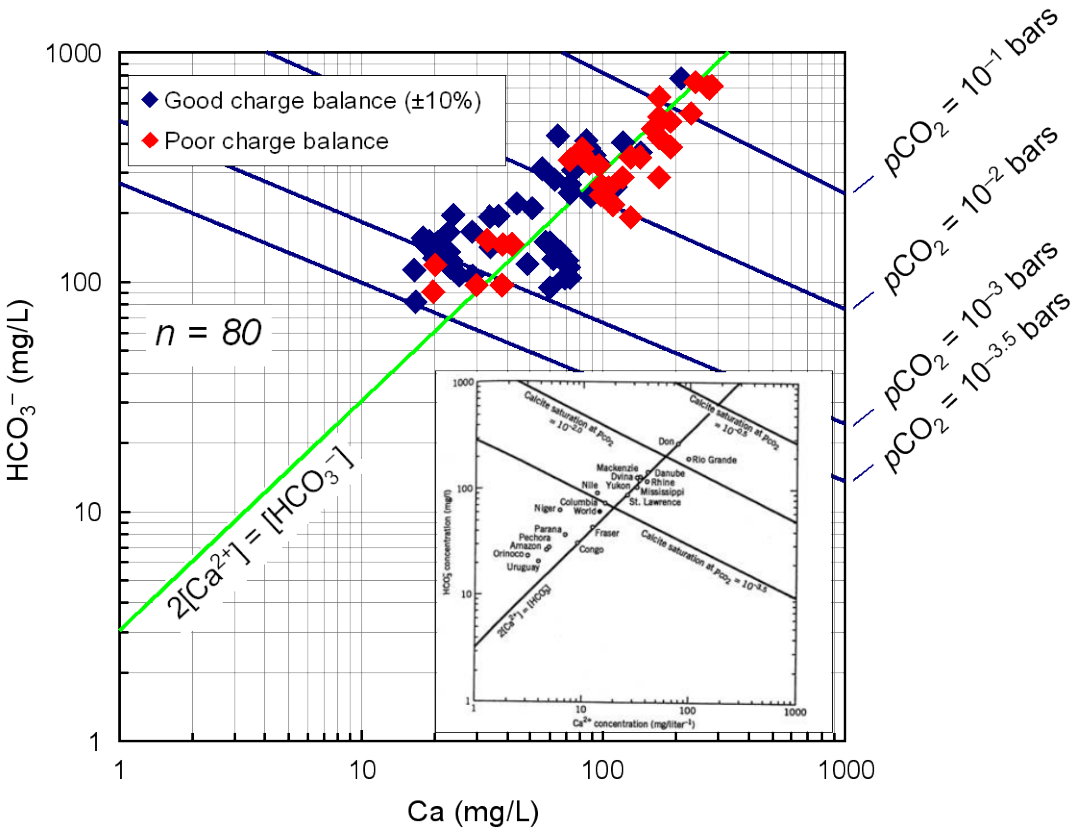

Source: Output DTN: SN0705PAEBSPCE.015, spreadsheet: *Results.xls*, tab: "Ca vs HCO3."

NOTE: Blue lines represent calcite saturation at the stated pCO_2 for the Ca-CO_2-H_2O system, calculated using EQ3 and data0.pce (Output DTN: SN0703PAEBSPCE.006). Insert from Stumm and Morgan 1996 [DIRS 125332], Figure 4.15.

Figure 6.6-8. Many TSw Pore Waters are Supersaturated with Respect to Calcite at a pCO_2 of 10^{-3} Bars

Detailed description of changes in response to CR 13647:

(1) Section 6.12.2.2.1, (pages 6-187 and 6-188):

In the last paragraph on page 6-187, replace:

The possible range of ambient feldspar dissolution rates can be evaluated by taking advantage of the knowledge that most of the alteration occurred at temperatures between 40°C and 100°C, with a maximum temperature of 180°C (Levy and O'Neil 1989 [DIRS 133364], p. 324), and also that there is a relationship between the ambient rate and the elevated temperature rate defined by the Arrhenius relationship (e.g., the 96°C rate is ~59 times the 23°C rate) (see the spreadsheet *Feldspar Dissolution Rate Calculations.xls* in Output DTN: SN0703PAEBSPCE.006).

With:

The possible range of ambient feldspar dissolution rates can be evaluated by taking advantage of the knowledge that most of the alteration occurred at temperatures between 40°C and 100°C, with a maximum temperature of 180°C (Levy and O'Neil 1989 [DIRS 133364], p. 324), and also that there is a relationship between the ambient rate and the elevated temperature rate defined by the Arrhenius relationship (e.g., the 100°C rate is ~59 times the 23.4°C rate) (see the File: WRIP calculations\Feldspar diss. rate calcs*Feldspar Dissolution Rate Calculations.xls*, tab "Arrhenius plot", in Output DTN: SN0703PAEBSPCE.006).

Later in that paragraph, on the top of page 6-188, replace:

This is because the temperature dependence of the feldspar dissolution rate, based on the Arrhenius relationship, is such that the rate at 96°C is 59 times the rate at 23°C (see the spreadsheet Feldspar Dissolution Rate Calculations.xls in Output DTN: SN0703PAEBSPCE.006).

With:

This is because the temperature dependence of the feldspar dissolution rate, based on the Arrhenius relationship, is such that the rate at 100°C is 59 times the rate at 23.4°C (see the File: WRIP calculations\Feldspar diss. rate calcs*Feldspar Dissolution Rate Calculations.xls,* tab "Arrhenius plot", in Output DTN: SN0703PAEBSPCE.006).

(2) Section 6.6.2, (page 6-87):

Replace the bullet:

- Eight perched water analyses from the base of the TSw were eliminated because they are Pleistocene in age (Yang, 2002 [DIRS 160839]) and do not represent current percolating water compositions.

With:

- Nine perched water analyses from the base of the TSw were eliminated because they are Pleistocene in age (Yang, 2002 [DIRS 160839]) and do not represent current percolating water compositions.

Detailed description of changes in response to CR 13655:

(1) Section 7.1.2.2, (pages 7-23):

Replace the existing Figure 7.1-6 with the following:

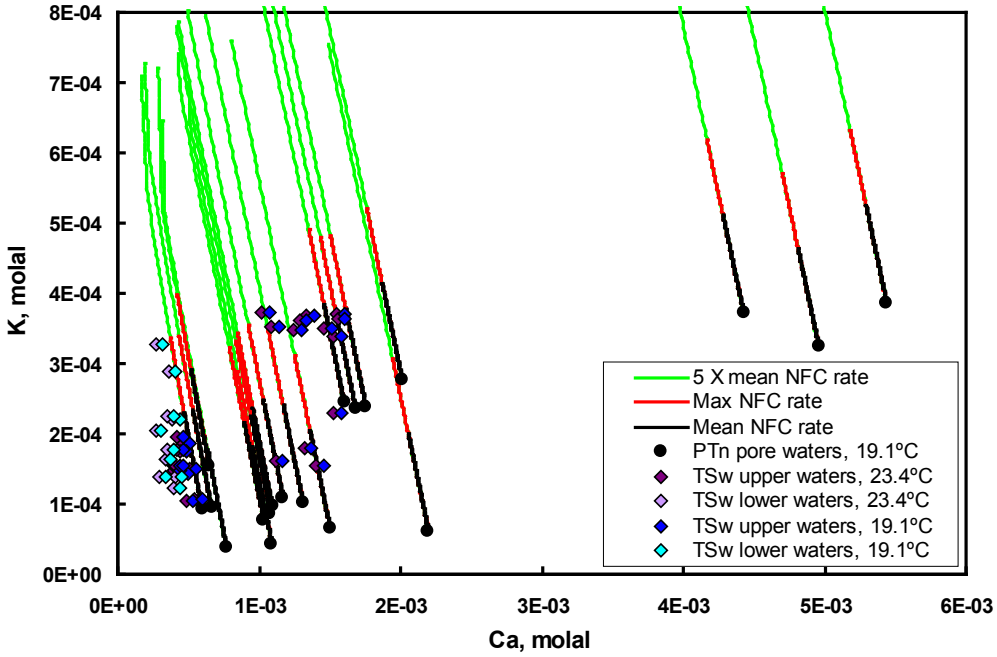

Source: Validation DTN: SN0705PAEBSPCE.014, File: Ambient pore waters*PTn-TSw equilibrated waters and results.xls*.

NOTE: TSw waters are shown equilibrated at both 19.1°C and 23.4°C, covering the likely range of applicable temperatures.

Figure 7.1-6. K versus Ca Molalities for TSw and PTn Pore Waters, Showing Predicted Evolutionary Pathways for the PTn Waters, at Three Different Feldspar Dissolution Rates

(2) Section 7.1.2.2, (pages 7-24):

Replace the existing Figure 7.1-7 with the following:

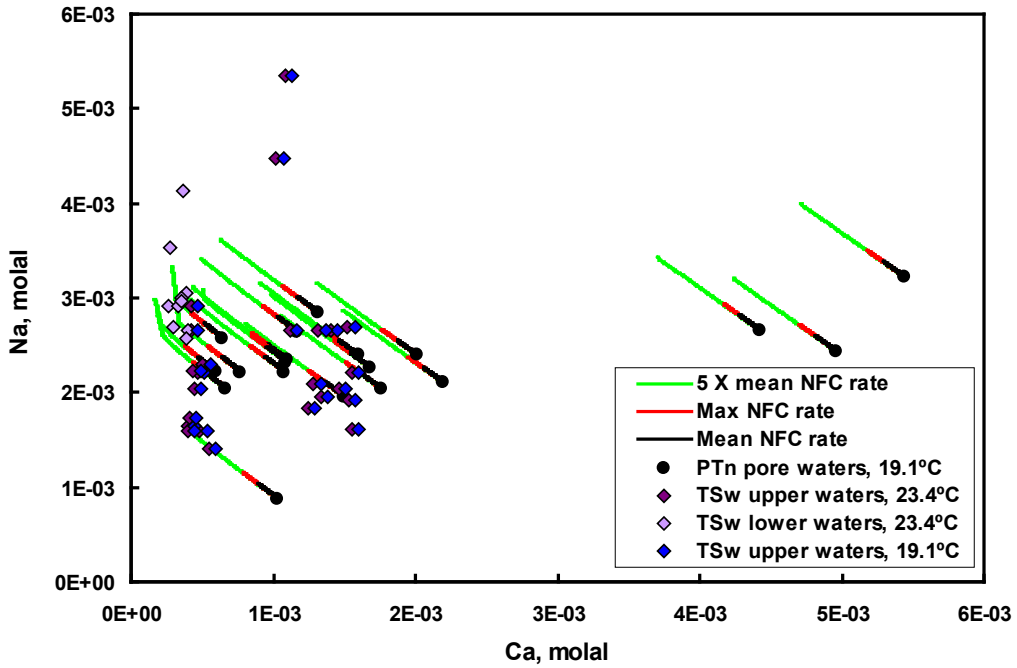

Source: Validation DTN: SN0705PAEBSPCE.014, File: Ambient pore waters*PTn-TSw equilibrated waters and results.xls*.

NOTE: TSw waters are shown equilibrated at both 19.1°C and 23.4°C, covering the likely range of applicable temperatures.

Figure 7.1-7. Plot of Na vs Ca Molalities for TSw and PTn Pore Waters, Showing Predicted Evolutionary Pathways for the PTn Waters, at Three Different Feldspar Dissolution Rates.

Required changes to the reference section (Section 9):

The following citations are added to Section 9.1 DOCUMENTS CITED

169855 BSC (Bechtel SAIC Company) 2004. *Development of Numerical Grids for UZ Flow and Transport Modeling.* ANL-NBS-HS-000015 REV 02. Las Vegas, Nevada: Bechtel SAIC Company. ACC: DOC.20040901.0001; LLR.20080522.0082; DOC.20090504.0002.

162561 Johnson, T.M. and DePaolo, D.J. 1996. "Reaction-Transport Models for Radiocarbon in Groundwater: The Effects of Longitudinal Dispersion and the Use of Sr Isotope Ratios to Correct for Water-Rock Interaction." *Water Resources Research, 32,* (7), 2203-2212. Washington, D.C.: American Geophysical Union. TIC: 252291.

177396 SNL 2007. *Radionuclide Transport Models Under Ambient Conditions.* MDL-NBS-HS-000008 REV 02 ADD 01. Las Vegas, Nevada: Sandia National Laboratories. ACC: DOC.20050823.0003; DOC.20070718.0003; DOC.20070830.0005; LLR.20080324.0002; DOC.20090114.0005; DOC.20090827.0003.

184614 SNL 2007. *UZ Flow Models and Submodels*. MDL-NBS-HS-000006 REV 03 AD 01. Las Vegas, Nevada: Sandia National Laboratories. ACC: DOC.20080108.0003; DOC.20080114.0001; LLR.20080414.0007; LLR.20080414.0033; LLR.20080522.0086; DOC.20090330.0026.

184748 SNL 2008. *Particle Tracking Model and Abstraction of Transport Processes*. MDL-NBS-HS-000020 REV 02 AD 02. Las Vegas, Nevada: Sandia National Laboratories. ACC: DOC.20080129.0008; DOC.20070920.0003; LLR.20080325.0287; LLR.20080522.0170; LLR.20080603.0082; DOC.20090113.0002.

105043 Sudicky, E.A. and Frind, E.O. 1982. "Contaminant Transport in Fractured Porous Media: Analytical Solutions for a System of Parallel Fractures." Water Resources Research, 18, (6), 1634-1642. Washington, D.C.: American Geophysical Union. TIC: 217475.

162133 Zhou, Q.; Liu, H-H.; Bodvarsson, G.S.; and Oldenburg, C.M. 2003. "Flow and Transport in Unsaturated Fractured Rock: Effects of Multiscale Heterogeneity of Hydrogeologic Properties." *Journal of Contaminant Hydrology, 60,* ([1-2]), 1-30. New York, New York: Elsevier. TIC: 253978.

The following citations are added to Section 9.2 SOURCE DATA, LISTED BY DATA TRACKING NUMBER

159525 LB0205REVUZPRP.001. Fracture Properties for UZ Model Layers Developed from Field Data. Submittal date: 05/14/2002.

179180 LB0610UZDSCP30.001. Drift-Scale Calibrated Property Set for the 30-Percentile Infiltration Map. Submittal date: 11/02/2006.

The following citations in Section 9.4 OUTPUT DATA, LISTED BY DATA TRACKING NUMBER are modified to reflect new submittal dates for the updated DTNs

SN0703PAEBSPCE.006. Physical and Chemical Environment (PCE) TDIP Water-Rock Interaction Parameter Table and Salt Separation Tables with Supporting Files. Submittal date: 9/23/2009.

SN0705PAEBSPCE.009. P&CE Normative Calculation of Mineral Abundances and Other Supporting Miscellaneous Calculations. Submittal date: 9/23/2009.

SN0705PAEBSPCE.015. P&CE Selection of Pore Water Data. Submittal date: 9/24/2009.

The following citations are added to Section 9.5 SOFTWARE CODES

146654 T2R3D V. 1.4. 1999. UNIX, WINDOWS 95/98NT 4.0. STN: 10006-1.4-00.

160242 TOUGH2 V. 1.6. 2002. DOS Emulation (win95/98), SUN OS 5.5.1, OSF1 V4.0. STN: 10007-1.6-00.

Description of changes to output DTNs:

DTN: SN0705PAEBSPCE.009: In response to CR 13343, the incorrectly parameterized FEHM simulations used in the previous AFM sensitivity analysis have been deleted. T2R3D input/output files, spreadsheet calculations, and other files supporting the impact analysis inserted into the document as Section 6.3.2.4.4.1 have been appended to this DTN. Finally, the *readme.doc* file for the DTN has been updated to include the additional files.

DTN: SN0703PAEBSPCE.006: In response to CR 13647, the calculation on tab "Arrhenius plot" of spreadsheet *Feldspar Dissolution Rate Calculations.xls*, has been corrected to accurately show the change in feldspar dissolution rate with temperature.

DTN: SN0705PAEBSPCE.015: In response to CR 13647, File *TSw_Porewater_Data.xls*, tab "All TSw." The lithologic unit designations for the perched water samples (spreadsheet rows 115–122) have been corrected. In addition (not related to CR 13647) the Q status of water samples from DTN: GS020808312272.004 was changed to "Q" on several tabs in spreadsheet *TSw_Porewater_Data.xls*, and on tab "Waters that meet criteria" of spreadsheet *Results.xls*, to reflect the changed status of that DTN in the TDMS.

Analysis of Impacted Documents:

The changes to ANL-EBS MD-000033 Rev. 06 that are documented in this ERD have no impact on the model conclusions or the model outputs that are used by the Total System Performance Assessment (TSPA). Hence, there is no impact to the TSPA. Also, none of the controlled documents which cite ANL-EBS-MD-000033 REV 06 reference the text or sections modified by this ERD. However, as documented in LCR 0141-00, several changes will be made to Chapter 2.3.5 of the LA Safety Analysis Report (LA SAR) in response to the changes in this ERD. Specifically, Section 2.3.5.3 of the SAR will be modified in three subsections (CR 13343) to reflect the new flow and transport analysis with T2R3D simulations; SAR Section 2.3.5.3.2.2.2 (p. 2.3.5-33) will be modified (CR 13647) to reflect three changes in cited temperature from 96ºC to 100ºC; and SAR Figure 2.3.5-22(a) will be updated (CR 13655) to correct the error in the zero values for the axes. No other sections of the SAR are affected.

The following is a list of documents citing ANL-EBS-MD-000033 REV 06 as a source:

Controlled Documents:

- ANL-EBS-GS-000001 Rev. 02
- ANL-EBS-MD-000003 Rev. 03
- ANL-EBS-MD-000004 Rev. 02, Add. 01
- ANL-EBS-MD-000037 Rev. 04, Add. 01
- ANL-EBS-MD-000038 Rev. 01
- ANL-EBS-MD-000049 Rev. 03, Add. 01
- ANL-EBS-MD-000049 Rev. 03, Add. 02
- ANL-EBS-PA-000011 Rev. 00
- ANL-EBS-PA-000012 Rev. 00
- ANL-NBS-HS-000047 Rev. 01
- ANL-NBS-HS-000057 Rev. 00
- ANL-WIS-MD-000010 Rev. 06
- ANL-WIS-MD-000024 Rev. 01
- ANL-WIS-MD-000027 Rev. 00
- ANL-WIS-MD-000027 Rev. 00, CAN 01
- ANL-WIS-PA-000001 Rev. 03
- MDL-EBS-MD-000001 Rev. 00, Add. 01
- MDL-EBS-PA-000004 Rev. 03
- MDL-NBS-HS-000001 Rev. 05
- MDL-NBS-HS-000020 Rev. 02, Add. 01
- MDL-WIS-PA-000005 Rev. 00
- TDR-PCS-SE-000001 Rev. 05, Add. 01
- LA GENERAL INFORMATION SECTION 5
- LA SAFETY ANALYSIS REPORT SECTION 1.1
- LA SAFETY ANALYSIS REPORT SECTION 2.3.5
- LA SAFETY ANALYSIS REPORT SECTION 2.3.6
- LA SAFETY ANALYSIS REPORT SECTION 2.3.7
- LA SAFETY ANALYSIS REPORT SECTION 2.3.11
- LA SAFETY ANALYSIS REPORT SECTION 2.4